Heliyon 11 (2025) e42439

Contents lists available at ScienceDirect

Heliyon

journal homepage: www.cell.com/heliyon

Research article

Electroforming-based micro-texturing: Advancements for surface engineering in EDM

Mariana Hernández-Pérez [a,*], Pedro M. Hernández-Castellano [a], Juan M. Vázquez-Martínez [b], María D. Marrero-Alemán [a]

[a] University of Las Palmas de Gran Canaria, Las Palmas de Gran Canaria, Spain
[b] University of Cádiz, Cádiz, Spain

ARTICLE INFO

Keywords:
Mask Stereolitography (MSLA)
Microtexturing
Electroforming
Surface microtopography
SEDM

ABSTRACT

In the domain of surface engineering, certain additive manufacturing technologies have established themselves as efficient and sustainable solutions. Mask stereolithography (MSLA) has gained prominence, especially when combined with the electroforming process for the production of microtextured copper electrodes. These electrodes are of particular interest in die sinking EDM (SEDM) applications, where high precision in geometry and microtextures is required, and alternative manufacturing technologies often struggle to meet these demands. This study presents the development of microtextured electrodes for sinking EDM processes (SEDM), fabricated by mask stereolithography (MSLA) and copper electroforming. The process starts with the design of textured 3D models using CAD software, followed by their fabrication with MSLA, using high-resolution photosensitive resins. Subsequently, the parts are metallized by sputtering to give them electrical conductivity and, finally, they are subjected to an electroforming process in an electrolytic bath to generate the copper shells. Finally, a metrological characterization was carried out at each stage of the process, from CAD design to the final part obtained by EDM, evaluating textures in low and high relief. The results demonstrate high replicability in the transfer of microtextures to electroformed shells. However, some dimensional variations are observed, primarily due to the inherent limitations of the resolution of MSLA technology. For biomimetic textures, such as those inspired by shark skin, excellent lateral fidelity was observed, while low-relief geometric textures presented greater variations due to the accumulation of photosensitive resin in the first layers of the texturing. Post-processing, particularly thorough cleaning using advanced techniques such as ultrasonic cleaning, proved crucial in minimizing dimensional errors and improving final accuracy. These findings provide a solid foundation for the development of future research aimed at optimizing the accuracy of electrode texturing for EDM applications, addressing a critical need in the field of functional surface microfabrication.

1. Introduction

Over the last century, advances in surface engineering have resulted from a broad understanding of how functional properties are

* Corresponding author.
E-mail addresses: mariana.hernandez@ulpgc.es (M. Hernández-Pérez), pedro.hernandez@ulpgc.es (P.M. Hernández-Castellano), juanmanuel.vazquez@uca.es (J.M. Vázquez-Martínez), mariadolores.marrero@ulpgc.es (M.D. Marrero-Alemán).

https://doi.org/10.1016/j.heliyon.2025.e42439
Received 17 December 2024; Received in revised form 1 February 2025; Accepted 1 February 2025
Available online 4 February 2025

influenced by surface properties. All surfaces possess textures and structures, some of which are explicitly engineered, while others are inherent in the nature of the materials or the forming processes to which they have been subjected [1]. Surface texture control has become increasingly important in modern engineering, especially in applications where precision and functional performance of surfaces are critical. In addition to the aesthetic benefits it can provide, texturing imparts functional properties to surfaces that optimize the behavior of devices and components in various industrial environments [2]. As these textures are miniaturized to the micro- and nanometer scale, they become even more relevant as they decisively influence key properties such as friction, adhesion, hydrophobicity and light scattering, fundamental aspects in sectors that require high precision [3]. As these textures are miniaturized to the micro- and nanometer scale, they become even more relevant as they decisively influence key properties such as friction, adhesion, hydrophobicity and light scattering, fundamental aspects in sectors that require high precision [4,5].

In the context of sinking EDM (SEDM) applications, surface textures designed for electrodes span a size range of typically 10–50 μm when fabricated by conventional methods such as chemical etching or micromachining. While these methods are widely used, they have significant limitations, such as high operational costs, generation of hazardous waste, and lack of flexibility to create complex patterns [6,7]. Conversely, emerging technologies such as mask stereolithography (MSLA) present a compelling alternative by enabling the fabrication of surface textures in the 20–200 μm range, offering enhanced versatility and reduced environmental impact. However, these technologies face inherent limitations, such as resolution restricted by the pixel size of the equipment (20–50 μm) and distortions caused by the accumulation of liquid resin in the initial layers [8].

Surface metrology has evolved to address these challenges, moving from a traditional focus on linear profiles to full surface area characterization [7,8]. This paradigm shift, which includes both stochastic and structured surfaces, has allowed for a better understanding of how surface topography influences device performance [9,10].

Among the methods that can be used to create textures, additive manufacturing (AM), specifically mask stereolithography (MSLA), has gained popularity for its ability to produce complex textured surfaces with extremely high levels of detail. However, the quality of the micro-textures produced is dependent on the precision of the equipment and the quality of the materials used. Limitations in display resolution and the need for rigorous post-processing pose significant challenges to achieving highly accurate functional surfaces [11]. An example of this is the use of ultrasonic cleaning techniques to remove resin residues that would limit the functionality of the textures. In this context, electroforming is emerging as an effective solution for the precise replication of complex geometries and surface textures. Electroforming is an electrolytic process used to produce metal parts of reduced thickness by controlled deposition of metal onto a model or pattern [12]. It is an essential process in several industrial applications that require high fidelity of detail, such as the manufacture of precision tools and micro-components [13]. The process starts with the preparation of a model part on which metal is deposited on its active surfaces, which must be electrically conductive to achieve metal deposition [14]. Once the required thickness is reached, the metal layer has its own integrity and is separated from the model part to obtain the final electroform [13,15,16].

Previous studies have explored the combination of MSLA and electroforming for the manufacture of tools for die sinking EDM (SEDM) and concluded that this combined process is feasible. High-precision textured electrodes can be obtained at low cost, with reasonable manufacturing time, and with a significant reduction in toxic waste generation compared to other traditional texturing methods. The main objective of this study is to enhance the reproducibility of electroforming micrometric-level textures generated by the MSLA process. The study is divided into two distinct phases. In the first phase, a synthetic description of a previous study is made to serve as a reference for the results and to present the main conclusions that guided the actions described in the second phase. In the second phase, the improvement of microtexture replicability through the implementation of complete cleaning protocols in MSLA

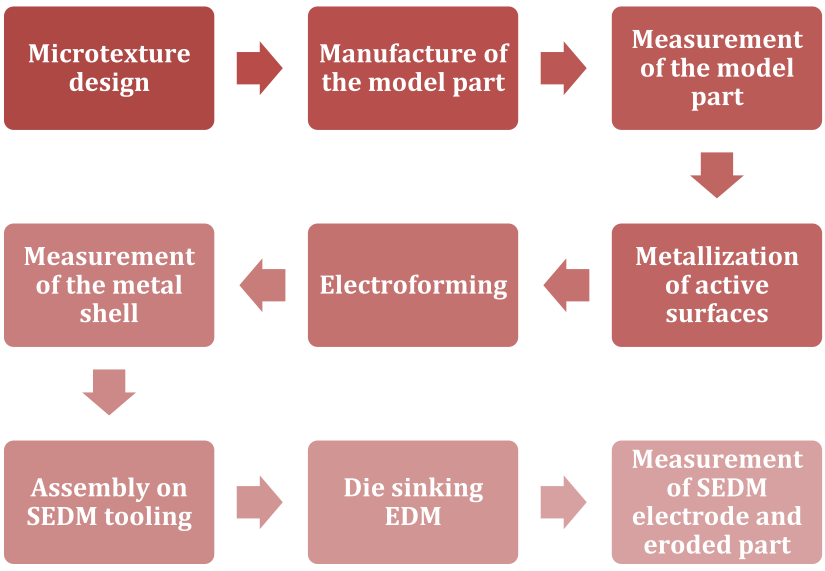

Fig. 1. Flow required for the production of electroformed SEDM electrodes.

technology is studied.

2. Materials y methods

2.1. Methodology for the development of electroformed SEDM electrodes

The SEDM electrode manufacturing process (see Fig. 1) begins with the design of model parts with textured surfaces, which are adjusted to align with the functional requirements and process capabilities. The model part is then manufactured using MSLA, with the appropriate operating parameters for the equipment and resin being set in advance. This technology requires post-processing for cleaning and curing. Once the plastic model part is obtained, it is necessary to metallize some of its surfaces in order to allow the passage of the electric current that produces the metal deposition in the electroforming process. To this end, the sputtering process is employed, enabling the deposition of a layer of a few nanometers on the active surfaces without affecting the geometry of the textures.

Once the model part is connected to the power supply and positioned correctly with the recirculation system, it can be introduced into the electrolytic bath. Once the program has been initiated, the electroforming process can begin. The power supply will then regulate the current and voltage parameters throughout the deposition stages. Once the total time established in the deposition program has elapsed, the process is concluded and the model part with the copper shell is removed from the bath. Prior to separating the shell from the model part, it is essential to reinforce it by filling the back side with an epoxy resin. This will prevent deformation during the separation process and facilitate assembly in the tooling designed for EDM. The equipment used in the two study phases of this project is outlined below.

2.2. Equipment and materials

2.2.1. Design of the model part

To carry out the first phase study it was necessary to generate the electroforms. To conduct the initial phase of the study, it was essential to create the electroforms. Accordingly, the requisite model parts were designed using the Fusion360 program with micrometric textures applied directly to the functional surface, enabling precise modeling of the desired patterns. Similarly, as illustrated in Fig. 2, a variety of micro textures were developed, which can be classified into three main groups: aesthetic, geometric, and biomimetic patterns. During the study, some textures were redesigned and parameterized to enhance replicability and functionality of the final pieces. This involved adjusting parameters such as maximum depth, pattern frequency, and texture orientation.

Fig. 1 illustrates the complete design of the model part, showcasing the active surfaces and the flat face where texturing is generated. The lower section presents a range of geometric patterns that can be incorporated into the central region of the model part.

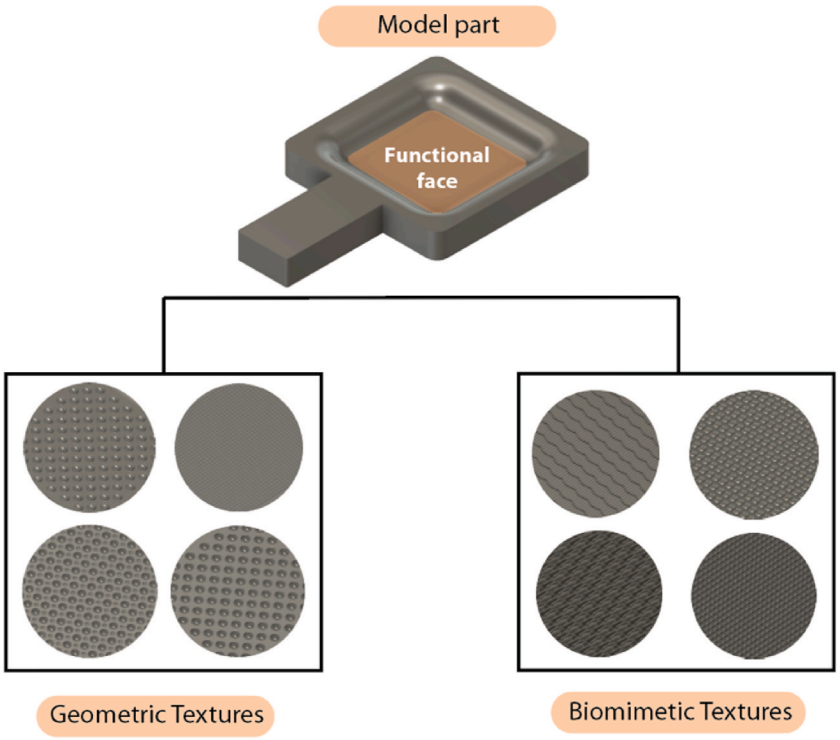

Fig. 2. Design of the model piece where the different textures will be applied.

To carry out the different studies that will be shown below, the textures of the geometric pattern of hemispheres and the biomimetic pattern of shark skin were selected. The former is a low relief texture and the latter is a high relief texture in order to evaluate if this aspect has an influence on the reproduction of textures at this scale. The selected textures and their main dimensions are shown in Fig. 3.

The texture composed of low relief hemispheres (Fig. 3a) may be suitable for a wide range of industrial applications, such as lubricant retention or reducing the contact area between components, among others [17]. In this texturing (Fig. 3a), composed of an 8 × 8 matrix and another 7 × 7 interleaved matrix, the value "a" represents the diameter of the hemisphere; "b" represents the distance between centers in the horizontal; "c" represents the distance between centers in the vertical; and "d" represents the depth or radius of the hemisphere. On the other hand, the second bio-inspired texture in over relief (Fig. 3b), was designed with an attempt to achieve a hydrophobic property on the surfaces. In this second texturing (Fig. 3b) with an 18 × 10 matrix and another interleaved matrix of 17 × 9, the value "a" represents the length of the scale; "b" represents the distance between the lateral ends in the horizontal; 'c' represents the distance between the lateral ends in the vertical and "d" represents the height of the scale.

2.2.2. *Manufacturing and post-processing of model parts*

For the manufacturing of the pieces, the first study used the Wanhao Duplicator 7 MSLA equipment, which offers a screen resolution of approximately 47 μm and allows working with a layer height of 50 μm. The material used was a commercial photosensitive resin of the same brand as the equipment, Wanhao 3D Printing Resin Clear, chosen for its transparency, which allowed the observation of the metal shell generation process in its early stages. For the second study, a more powerful MSLA machine, the Phrozen Mini 8K, was used, offering a screen resolution of 22 μm per pixel and layer heights of up to 10 μm, which represents a significant improvement in the level of detail of the geometric patterns that can be fabricated. The material used was Phrozen Aqua Red-Clay 8K photosensitive resin from the same manufacturer. The parameters used in each case are shown in Table 1, varying only the essential parameters required by the change in resin in order to make the comparison as reliable as possible.

In the first study, a manual cleaning protocol, as detailed in Table 2, was performed using only one curing station. In the second study, the post-processing of the parts was also significantly improved using new equipment. Isopropyl alcohol washing was enhanced by the use of Phrozen's Vortex Agitation Wash Station, complemented by Phrozen's Ultra-Sonic Cleaner ultrasonic cleaning equipment, which removed almost all resin residue from the textured surface. Drying and curing was enhanced with Phrozen's Cure Kit station, which completed the resin polymerization process. The cleaning protocols used in both studies, shown in Table 2, are detailed below to explore the influence of the different equipment used.

2.2.3. *Metallization*

The active surfaces were metallized using the Quorum Technologies SC7620 'Mini' sputtering system, which deposits a gold-palladium layer of a few nanometers thickness that does not alter the geometry of the textures. Two 120-s depositions were performed at 18 mA to ensure metallization of the entire textured surface.

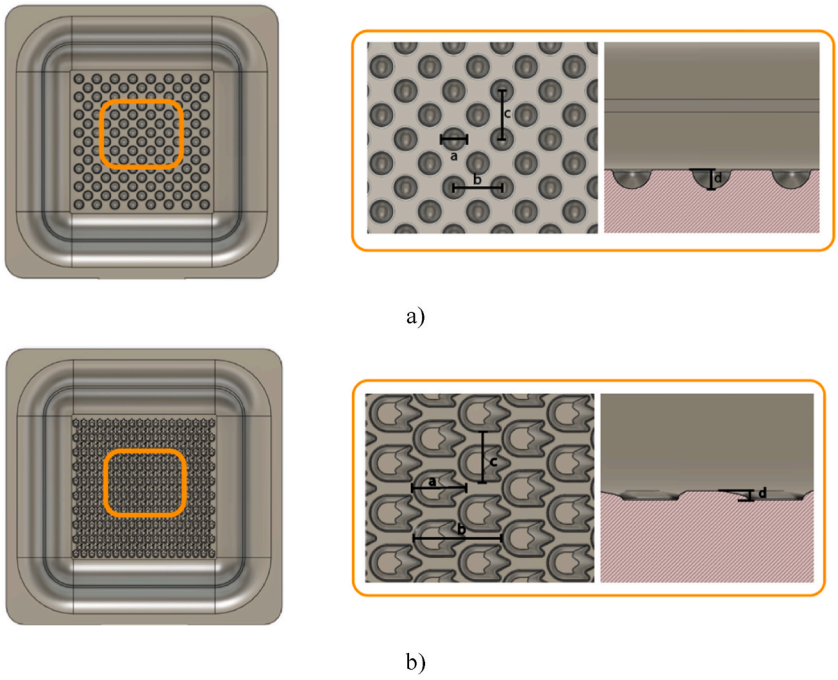

Fig. 3. a) Design and composition of the geometric texture under relief; b) Design and composition of the biomimetic texture on relief.

Table 1
Technical specifications for printing with different equipment.

Parameters	Parameters	Values	
		Wanhao	Phrozen
Basic information	Layer height (μm)	50	50/25
	Retraction speed (mm/min)	150	150
Undercoats	Nº of layers	4	4
	Exposure time(s) (seg)	40	35
	Lifting distance (mm)	6	6
	Lifting speed (mm/min)	60	60
Normal layers	Exposure time(s) (seg)	10	2
	Lifting distance (mm)	6	6
	Lifting speed (mm/min)	60	60
Waiting during printing	Rest time after retracting (seg)	3	3

Table 2
Cleaning protocols employed in the study.

Stages	1	2	3	4	5
Protocols	Pre-separation of the model part	Cleaning with isopropyl alcohol	Ultrasonic cleaning	Drying	Curing
Original Manual Cleaning (MC)	Yes	Manual spraying	No	Pressurized air	2 min
Manual Cleaning (MC)	Yes	Manual spraying	No	Automatic station drying	2 min
Power Assisted Cleaning (AM)	No, it remains on the platform	2 min in washing station	Yes	Pressurized air	2 min

2.2.4. *Electroforming*

The experimental laboratory equipment used for electroforming was developed specifically for this research project. The main components are shown in Fig. 6. These were defined in detail in the work of Sánchez Morales, C.J [18]. The Bright Copper Plating Bath CU 501 electrolytic copper bath, produced by the Heimerle-Meule company, was used. The power supply used is the Keithley 2460 SourceMeter, which enables the programming of distinct stages with both constant voltage and constant current. Following several trials, a program comprising four stages of increasing intensity was established to achieve a gradual and complete deposition of the geometric details and textures. The total time required for the elaboration of the shells was 240 min, resulting in an average thickness of 0.3 mm.

2.2.5. *Metrological characterization*

For the metrological characterization studies, the Alicona InfiniteFocusG5+ variable focus microscope available at the Metrology Laboratory of the University of Cadiz, shown in Fig. 4, was used. It allows the measurement of several geometric features in the sub-micron range with a maximum resolution of 10 nm in the vertical direction, which allows the measurement of roughness in the order of 30 nm. The software used to analyze the results obtained is MountainsMap, developed for the analysis of surface microtopography [19].

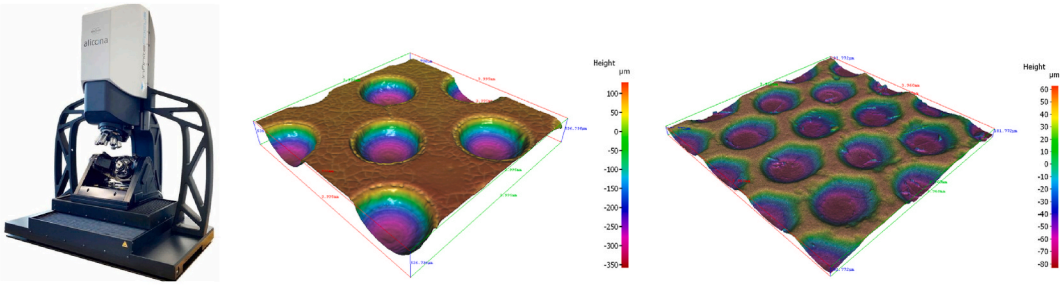

Fig. 4. a) Alicona InfiniteFocusG6 variable focus microscope; b) three-dimensional topography of incoming hemisphere texture; c) three-dimensional topography of shark skin texture.

3. Results

This section details the results of the two studies presented in this paper, highlighting the most relevant aspects.

3.1. Phase 1. study of dimensional deviation in the fabrication of microtextured EDM electrodes

This section summarizes the key findings from the previous work on dimensional deviation analysis at all stages of the electroformed electrode manufacturing process. The main sources of error were identified in the nominal reference dimensions established in the CAD of the model part, shown in Fig. 6a and b, in the fabricated model part, in the electroformed copper shell, and in the final dimensions in the EDM part.In this study, the average values of 10 measurements were calculated for each size, obtained from the information provided by variable focus microscopy. This manual measurement process was carried out using the MountainsMap software, and the standard deviations of the corresponding samples were determined. The results obtained are presented in Tables 3 and 4.

It was concluded that the main source of error is in the manufacturing of the model part, mainly in the parameter “a", which defines the reference dimension of the texture generator element, and the parameter “d", which defines the height of the generator element.

It was concluded that the main source of error is in the fabrication of the model part, due to the resolution of the screen of the device on the one hand, and the overexposure of the liquid resin adhering to the surfaces during the fabrication of the subsequent layers on the other hand. With a pixel size of 47 μm of the MSLA device used, a minimum matrix of 25 × 25 pixels is required to define the circular geometry of the element generating the hemispherical texture. If this regular shape is not well centered in the matrix, significant distortions of the original shape are generated, as shown in Fig. 5. The geometry of the biomimetic texture generator element is more irregular, and the geometric distortion can be proportionally greater in the areas of lower dimensional detail closer to the pixel size.

Regarding the geometric distortion caused by the liquid resin that remains adhered to the solidified surfaces, this resin receives a new light exposure when the new layer is generated, so that part of it solidifies as well. This distortion is influenced by the ease with which the resin moves when the building platform is moved, so that it is more pronounced in geometries that create traps. Low relief microstructures are likely to be more affected by this phenomenon than high relief microstructures (Fig. 6a). During the MSLA fabrication process, the combined effect of these two phenomena occurs, producing an amplification of these geometric distortions. Added to this is the possible lack of repeatability in the horizontal positioning of the construction plate during the up and down movements of the same, influenced by the mechanical solutions of these mechanisms and their state of conservation (Fig. 6b).

Therefore, as can be seen from the results in Tables 1 and 2, the error variance in the fabrication of the copper shell by electroforming and in the fabrication of the EDM part are very small compared to those obtained in the fabrication of the model part. This clearly indicates that the replication capability of both processes is far superior to that of the MSLA process used.

3.2. Phase 2. improvement in the manufacturing of the model parts

Based on the results of the preliminary study, it was identified that the manufacturing stage of the model parts using MSLA was critical to improve the replicability of the proposed process. For this reason, it was decided to acquire a higher performance equipment, the Phrozen Mini 8K complemented with advanced post-processing systems, as indicated in section 2.

With this new equipment, it was decided to keep the same textures described in Phase 1 in order to make a more reliable comparison of the results. We wanted to analyze in detail the influence of the cleaning phase of the model parts prior to curing in order to define a procedure that would allow us to achieve the highest possible level of detail. In order to make a direct comparison with the results obtained in Phase 1, it was decided to first maintain a manual cleaning process as used in that phase and then compare it with the cleaning protocols already described in the Materials section. Also, with this new equipment, we wanted to work with layer heights of 25 μm, half the value used in the first phase, in order to improve the vertical resolution of the textures generated.

The introduction of this process for producing textured model parts of higher quality has made it possible to achieve a higher level of definition in the textures, as can be seen in Figs. 7 and 8, where the surface topography measured by the variable focus microscope is shown.

The point cloud obtained with the variable focus microscope allows to perform measurements with the MountainsMap software, developed for the analysis of the microtopography of 3D surfaces. Tables 5 and 6 show the results of the measurement process of the

Table 3
Metrological characterization of the low relief semisphere texture generation process.

Low relief semisphere texture										
		PHASE 1: Model Part			PHASE 2: Copper Shell			PHASE 3: Eroded Piece		
D [mm]	CAD [mm]	Av. [mm]	S.D. [mm]	Error 1 [mm]	Av. [mm]	S.D. [mm]	Error 2 [mm]	Av. [mm]	S.D. [mm]	Error 3 [mm]
a	**1.2**	1.142	0.038	0,058	1.111	0.014	0,089	1.149	0.020	0,051
b	**2.5**	2.509	0.010	−0,009	2.515	0.015	−0,015	2.518	0.009	−0,018
c	**2.5**	2.513	0.011	−0,013	2.515	0.012	−0,015	2.508	0.017	−0,008
d	**0.6**	0.401	0.014	0,199	0.458	0.021	0,142	0.443	0.004	0,157

D: Dimension; S.D.: Standard Deviation; Av.: Average; Error 1 = CAD – Av.P.M.; Error 2 = CAD – Av.C.C.; Error 3 = CAD – Av.P.E.

Table 4
Metrological characterization of shark skin textures generation process.

Shark skin texture										
		PHASE 1: Model Part			PHASE 2: Copper Shell			PHASE 3: Eroded Piece		
D [mm]	CAD [mm]	Av. [mm]	S.D. [mm]	Error 1 [mm]	Av. [mm]	S.D. [mm]	Error 2 [mm]	Av. [mm]	S.D. [mm]	Error 3 [mm]
a	**1.21**	1042	0,031	0,168	1056	0,029	0,154	1065	0,032	0,145
b	**2.00**	2047	0,021	−0,047	2051	0,016	−0,051	2040	0,014	−0,040
c	**1.10**	1136	0,020	−0,036	1119	0,037	−0,019	1117	0,027	−0,017
d	**0.15**	0,128	0,005	0,022	0,139	0,005	0,011	0,131	0,004	0,019

D: Dimension; S.D.: Standard Deviation; Av.: Average; Error 1 = CAD – Av.P.M.; Error 2 = CAD – Av.C.C.; Error 3 = CAD – Av.P.E.

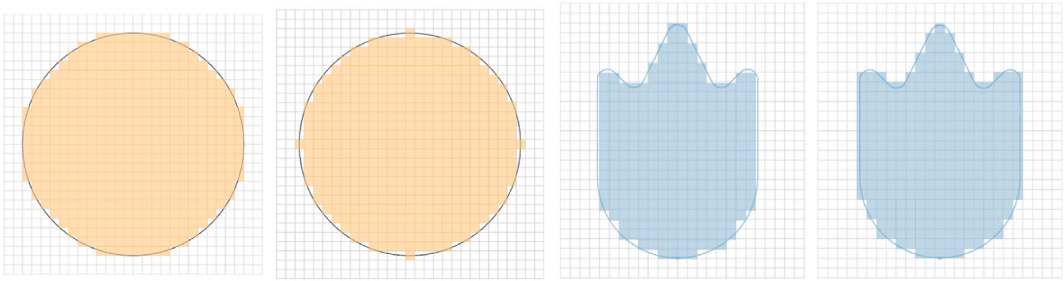

Fig. 5. Representation of dimension distortion attributed to the 3D printer screen resolution.

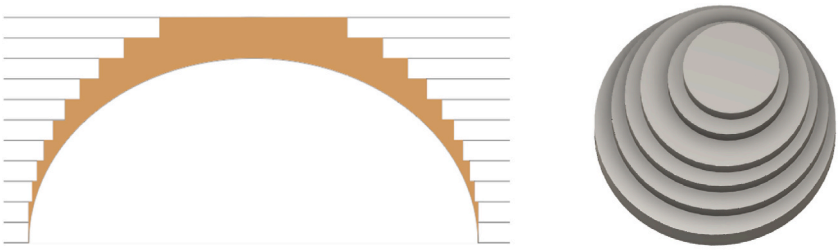

Fig. 6. a) Resin entrapment in incoming geometry; b) Error generated by the construction plate.

parameters defining the textures, “a", “b", “c" and “d", for the 4 cases of analysis mentioned. The same procedure was used to obtain the mean and the standard deviation of a sample of 10 measurements. For the first three values, the measurement is constrained within a box and for the “d" value, the study of the peaks/valleys present in the software is used. It is observed that the errors are drastically reduced when the assisted cleaning is applied, and a significant error reduction is also observed when the accuracy of the MSLA equipment is improved by maintaining a manual cleaning procedure.

In the case of the texture of the hemispheres in low relief, no significant differences were observed when a manual cleaning process

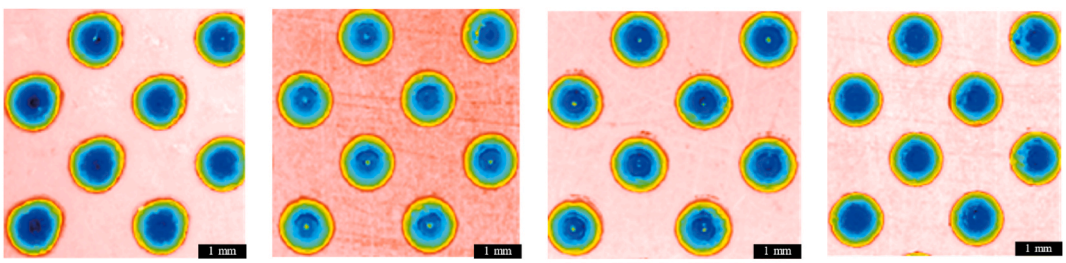

Fig. 7. Texture resolution of hemispheres as a function of cleaning protocol, layer height and equipment resolution.

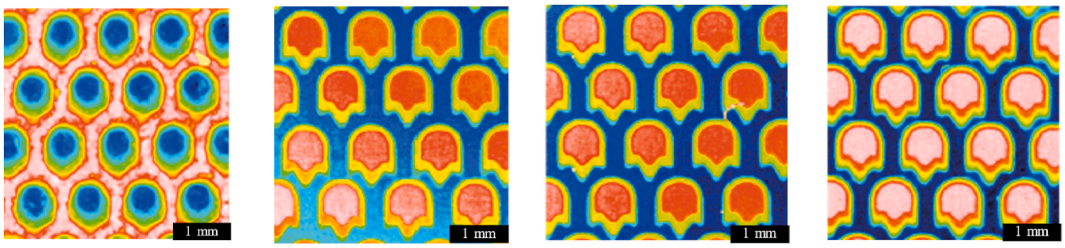

Fig. 8. Shark skin texture resolution as a function of cleaning protocol, layer height and equipment resolution.

Table 5
Metrological characterization of the low relief semisphere texture cleaning process.

Low relief semisphere texture												
D	CAD	MC_50_original			MC_50			AC_50			AC_25		
		Av	S.D.	Error 1	Av	S.D.	Error 2	Av	S.D.	Error 3	Av	S.D.	Error 4
a	**1200**	1142	0,038	0,058	1136	0,016	0,064	1163	0,015	0,037	1170	0,016	0,030
b	**2500**	2509	0,01	0,009	2518	0,022	0,018	2501	0,003	0,001	2503	0,005	0,003
c	**2500**	2513	0,011	0,013	2512	0,020	0,012	2506	0,005	0,006	2506	0,005	0,006
d	**0,600**	0,401	0,014	0,199	0,468	0,016	0,132	0,601	0,003	0,001	0,586	0,008	0,014

D: Dimension; S.D.: Standard Deviation; Av.: Average; Error 1 = CAD – Av.O. (50 μm).; Error 2 = CAD – Av.M.C. (50 μm); Error 3 = CAD – Av.C.C. (50 μm).; Error 4 = CAD – Av.C.C. (25 μm).

Table 6
Metrological characterization of shark skin textures cleaning process.

Shark skin texture												
D	CAD	MC_50_original			MC_50			AC_50			AC_25		
		Av	S.D.	Error 1	Av	S.D.	Error 2	Av	S.D.	Error 3	Av	S.D.	Error 4
a	**1160**	1042	0,031	0,168	1151	0,017	0,009	1154	0,008	0,006	1164	0,010	0,004
b	**2060**	2047	0,021	0,047	2064	0,024	0,004	2064	0,010	0,004	2058	0,010	0,002
c	**1100**	1136	0,02	0,036	1100	0,006	0,000	1100	0,000	0,000	1100	0,000	0,000
d	**0,150**	0,128	0,005	0,022	0,141	0,007	0,009	0,153	0,002	0,003	0,149	0,004	0,001

D: Dimension; S.D.: Standard Deviation; Av.: Average; Error 1 = CAD – Av.O. (50 μm).; Error 2 = CAD – Av.M.C. (50 μm); Error 3 = CAD – Av.C.C. (50 μm).; Error 4 = CAD – Av.C.C. (25 μm).

was applied, but very significant differences were observed when the assisted cleaning process was applied. However, for the biomimetic texture in high relief, the errors in all phase 2 textures are much lower than the phase 1 reference texture. This is possibly due to the greater ease of resin movement in these over-relief textures, where the chances of entrapment are much lower.

Contrary to what happens with the sharkskin texture, the error in the “f" dimension in the cleaning protocol for layer heights of 25 μm, although lower than in the manual cleaning protocols, still maintains a relatively high value with respect to the other dimensions (around 15 μm) in the hemisphere texture. This behavior could be related to the curved geometry of the texture, where the identification of the measuring points is more complex.

In addition, a similar situation, although to a lesser extent, is observed in dimension “a", where the error in AC_50 and AC_25 is practically half of that in the manual cleaning protocol. This can be explained by the longer curvature of the spheres, which could cause difficulties in the accurate detection of the end line for the measurements. The algorithms used for edge detection could have limitations when faced with curved surfaces, increasing the possibility of errors in the dimensional calculation.

For the shark skin texture, the implementation of the new equipment made a significant difference, significantly reducing the errors for the different dimensions analyzed. In addition, by applying more thorough cleaning methods and reducing the layer height, the errors decreased significantly, reaching minimal differences compared to the CAD model, with variations of only 4 μm.

In conclusion, the study has shown a significant improvement in the resolution and geometric accuracy of the evaluated textures between Phase 1 and Phase 2, which is reflected in the reduction of the average dimensional error in all analyzed parameters. For the hemispherical textures, the average error of the “a" dimension was reduced from 0.058 mm in Phase 1 (MC_50_original) to 0.030 mm in Phase 2 (AC_25), an improvement of 48.3 %. The “d" dimension showed the greatest improvement, going from an error of 0.199 mm in Phase 1 to 0.014 mm in Phase 2, a reduction of 92.9 %. Similarly, in the shark skin texture, dimension “a" showed a reduction in error from 0.168 mm (MC_50_original) to 0.004 mm (AC_25), an improvement of 97.6 %. Finally, dimension “d" experienced a reduction in error from 0.022 mm to 0.001 mm between the two phases, achieving a reduction of 95.5 %. These results underline the effectiveness

of the improvements implemented in the technology and process protocols.

4. Discussion

This previous study also analyzed the dimensional variation of the copper shell after the EDM process under finishing conditions with a very low VDI. The aim was to evaluate the wear experienced by the electrode, obtaining variations in the order of a few microns, observing that the most significant variations were due to the adhesion of particles of the eroded material or to possible deformations due to the temperatures reached during the EDM process.

The results obtained are in agreement with the study of Acharya et al. which confirms that electroformed copper electrodes have a high potential for application in EDM processes under finishing conditions, where controlled wear is sought to achieve high precision [20]. This is what is sought in the functional texturing of surfaces by providing those geometric elements that achieve certain properties.

After analyzing the results presented in this work, it can be concluded that the reproducibility of the microtextures studied has improved significantly. In Phase 1, it was found that the main limitation was the manufacturing process of the model parts by MSLA. Likewise, a visual inspection was carried out with the Olympus BX51 fluorescence microscope, which showed a very high capacity of replication in the electroforming process, regardless of the type of texture (Fig. 9). This confirms that the choice of the sputtering process for plating the active surfaces of the model parts does not cause any significant geometric distortion of the microtextures.

Post-processing, specifically the cleaning phase prior to curing, has a very significant impact on the dimensional accuracy of parts manufactured using technologies such as MSLA, especially when geometric details in the micrometer range are to be generated. This aspect has been highlighted by several previous studies, such as Trieu et al. who analyzed the post-processing of stereolithography parts and observed that electrolytic cleaning had a direct effect on the consistency of the layer thickness, resulting in more accurate parts with less deformation [21]. Similarly, Chen et al. investigated post-processing in 3D printing to improve the accuracy of ceramic membranes and concluded that thorough cleaning is critical to minimize dimensional errors associated with residual resin buildup [22].

The use of high-resolution MSLA equipment makes it possible to reduce the size of the texture-generating elements. The Phrozen Mini 8K equipment would make it possible to obtain textures with the same level of detail as those obtained with the Wanhao Duplicator 7 equipment used in Phase 1, but with a dimension almost 5 times smaller. If we add to this the use of much more efficient assisted cleaning systems, such as those used in Phase 2 of this work, the same textures can be obtained with a parameter “a" of the generator element around 250 μm. This would also imply a much larger file size needed for additive manufacturing, as the mesh would be much more refined.

For this reason, we have proposed a geometric simplification of the elements generating the textures, adapting them to the construction capabilities of the available MSLA equipment. In the geometries proposed in this study, we have thought of modeling the hemisphere by successive extrusion cuts of discs of variable diameter and height equal to the thickness of the layer to be used in the manufacturing process. In the case of the sharkskin texture, it would be modeled by superimposing two-dimensional contours with the thickness of the layer height (Fig. 10). At these scales, the manufacturing process itself creates edge rounding that smooth the geometries without the need to introduce these features into the modeling. This strategy allows for a significant reduction in the weight of the digital files without losing the ability to define the geometries in detail.

To achieve more realistic biomimetic textures, a parameterization of the geometry of the generating elements has also been implemented to apply variable orientation and distortion factors in three dimensions. In this way it is possible to generate more organic textures, as in the example of the shark skin, with scales of different sizes and orientations, as shown in (Fig. 10a), for which the Grasshopper module of the Rhinoceros application was used.

In addition, preliminary tests have been conducted with bio-inspired shark skin textures applied by erosion to aluminum sheets to evaluate their functional properties. The results have shown significant hydrophobic behavior, reaching contact angles above 100°, reinforcing the potential of these textures in applications where water resistance is critical. Moreover, this value is improved by

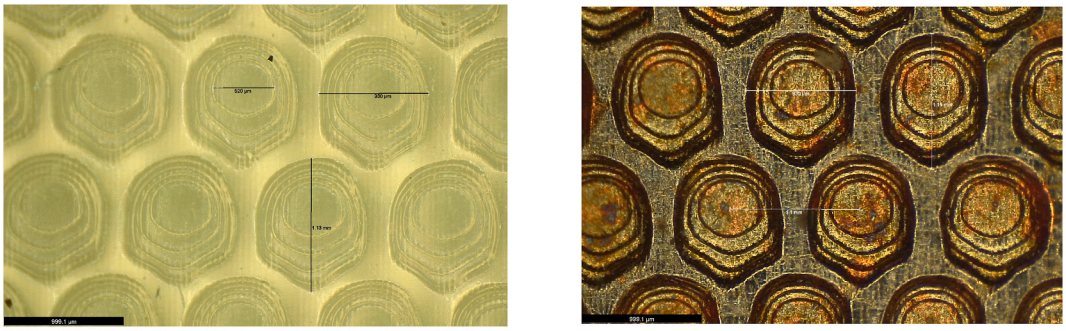

a) Model part analysis *b) Electroform analysis*

Fig. 9. Texture analysis of incoming hemispheres in resin model part and in copper shell.

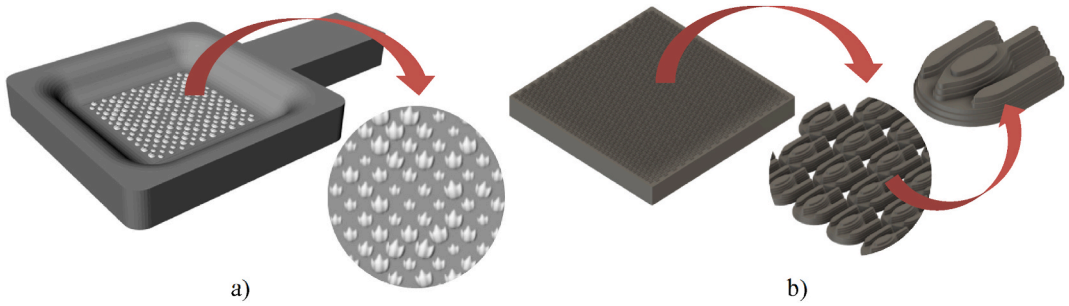

Fig. 10. Optimization of shark skin texture by parameterization. a) Form parameterization; b) Slicer of the scale (700 × 500 × 225mm).

reducing the size of the flakes. In subsequent projects, we plan to enhance this behavior by implementing a strategy to minimize the size of the microtextures.

Concurrently, we are developing a method to improve the electroforming process. This method will analyze the impact of various operative parameters on the uniformity of the thickness of the metallic deposition of copper. The objective is to produce electrodes capable of functioning under finishing conditions with more challenging EDM parameters.

5. Conclusions

This work demonstrates the great potential of the use of copper electrodes for spark erosion (SEDM), developed from a combined process of electroforming and mask steoreolithography additive manufacturing (MSLA) technology. It is an efficient and economical alternative for the production of tools for surface texturing. These electrodes enable the creation of micron-scale surface textures with complex geometries that are difficult or impossible to achieve using conventional processes. In addition, the manufacturing times of these tools can be reduced, making them an attractive option compared to alternative processes.

It has been possible to limit and quantify the dimensional deviations in the manufacturing process and to achieve a high reproducibility of the textures by electroforming. This allows these dimensional variations to be taken into account in the early stages of designing the geometric patterns of the electrodes. A higher level of detail is achieved in the functional texturing of surfaces that provide improved properties.

It has been found that the major source of dimensional error in the process is the MSLA fabrication phase of the model parts required for the electroforming process. The introduction of high-resolution equipment and more efficient post-processing systems has improved the ability to replicate geometric microstructures. In particular, the study has shown that the cleaning phase of the resin residues on the surface of the model parts is critical to achieve geometric details at the micrometer level.

CRediT authorship contribution statement

Mariana Hernández-Pérez: Writing – review & editing, Writing – original draft, Visualization, Validation, Supervision, Software, Resources, Project administration, Methodology, Investigation, Funding acquisition, Formal analysis, Data curation, Conceptualization. **Pedro M. Hernández-Castellano:** Writing – review & editing, Visualization, Validation, Supervision, Resources, Project administration, Formal analysis, Conceptualization. **Juan M. Vázquez-Martínez:** Writing – review & editing, Software, Resources, Investigation, Data curation. **María D. Marrero-Alemán:** Writing – review & editing, Validation, Supervision, Methodology, Conceptualization.

Data availability statement

Data included in article/supp. material/referenced in article.

Additional information

No additional information is available for this paper.

Funding statement

Work co-financed by the Agencia Canaria de Investigación, Innovación y Sociedad de la Información de la Consejería de Economía, Conocimiento y Empleo y por el Fondo Social Europeo (FSE) Programa Operativo Integrado de Canarias 2014–2020, Eje 3 Tema Prioritario 74 (85 %).

Declaration of competing interest

The authors declare that they have no known competing financial interests or personal relationships that could have appeared to influence the work reported in this paper.

References

[1] C.J. Evans, J.B. Bryan, Structured', 'textured' or 'engineered' surfaces, CIRP Annal. 48 (2) (Jan. 1999) 541–556, https://doi.org/10.1016/S0007-8506(07)63233-8.

[2] O. Bilek, J. Ondrik, P. Janik, T. Kautsky, Microtexturing for enhanced machining: evaluating tool performance in Laser-processed cutting inserts, Manufact. Technol. 24 (2) (Apr. 2024) 173–182, https://doi.org/10.21062/mft.2024.038.

[3] D.S. Wiersma, The physics and applications of random lasers, Nat. Phys. 4 (5) (May 2008) 359–367, https://doi.org/10.1038/nphys971.

[4] A.A.G. Bruzzone, H.L. Costa, P.M. Lonardo, D.A. Lucca, Advances in engineered surfaces for functional performance, CIRP Annal. 57 (2) (Jan. 2008) 750–769, https://doi.org/10.1016/j.cirp.2008.09.003.

[5] N. Moronuki, Tokyo Metropolitan University, Functional texture design and texturing processes, Int. J. Autom. Technol. 10 (1) (Jan. 2016) 4–15, https://doi.org/10.20965/ijat.2016.p0004.

[6] F.-T. Weng, Fabrication of microelectrodes for EDM machining by a combined etching process, J. Micromech. Microeng. 14 (Mar. 2004) N1, https://doi.org/10.1088/0960-1317/14/5/N01.

[7] K.M.T. Ahmmed, C. Grambow, A.-M. Kietzig, Fabrication of Micro/Nano Structures on Metals by Femtosecond Laser Micromachining, vol. 5, 2014, https://doi.org/10.3390/mi5041219.

[8] A. Darulis, "The Complete Resin 3D Printing Settings Guide for Beginners," AmeraLabs. Accessed: January. 28, 2025. [Online]. Available: https://ameralabs.com/blog/the-complete-resin-3d-printing-settings-guide-for-beginners/.

[9] R. Leach, H. Haitjema, R. Su, A. Thompson, Metrological characteristics for the calibration of surface topography measuring instruments: a review, Meas. Sci. Technol. 32 (3) (Dec. 2020) 032001, https://doi.org/10.1088/1361-6501/abb54f.

[10] A. Townsend, N. Senin, L. Blunt, R.K. Leach, J.S. Taylor, Surface texture metrology for metal additive manufacturing: a review, Precis. Eng. 46 (Oct. 2016) 34–47, https://doi.org/10.1016/j.precisioneng.2016.06.001.

[11] Z. Xing, H. Zhou, W. Liu, J. Nie, Y. Chen, W. Li, Efficient cleaning of ceramic green bodies with complex architectures fabricated by stereolithography-based additive manufacturing via high viscoelastic paste, Addit. Manuf. 55 (Jul. 2022) 102809, https://doi.org/10.1016/j.addma.2022.102809.

[12] J.A. McGeough, M.C. Leu, K.P. Rajurkar, A.K.M. De Silva, Q. Liu, Electroforming process and application to micro/macro manufacturing, CIRP Annal. 50 (2) (Jan. 2001) 499–514, https://doi.org/10.1016/S0007-8506(07)62990-4.

[13] H.G. Knol, C.J. Kruithof, C.J.M.V. Rijn, W. Nijdam, Electroforming method, electroforming mandrel and electroformed product. https://patents.google.com/patent/EP0894157A1/en, Feb. 03, 1999. (Accessed 6 October 2024).

[14] W.G. Herbet, T. Nozaki, A. Onishi, Electroforming apparatus and process. https://patents.google.com/patent/US4781799A/en, 1988. (Accessed 6 October 2024).

[15] P.W. Buckley, D.J. Coyle, M.J. Davis, R. Edwards, K.P. Zarnoch, Electroform, methods of making electroforms, and products made from electroforms. https://patents.google.com/patent/WO2007064804A1/en, Jun. 07, 2007. (Accessed 6 October 2024).

[16] D.G. DuPree, Electroforming an endless flexible seamless xerographic belt. https://patents.google.com/patent/US3954568A/en, May 04, 1976. (Accessed 6 October 2024).

[17] J.D.J. Reséndiz-Pérez, Enhancing Tribological Properties of Metallic Sliding Surfaces through Micro Multi-Texturing Techniques, University of Calgary, Canada, 2019. Doctoral Thesis, https://prism.ucalgary.ca/handle/1880/110625. (Accessed 8 October 2024).

[18] C.J. Sánchez Morales, Desarrollo de un equipo de Micro-Electroconformado. Estudio experimental de aplicación a la fabricación de herramientas para el texturizado de superficies estructuradas, Doctoral Thesis, ULPGC, Spain, https://accedacris.ulpgc.es/jspui/handle/10553/111011, 2021. (Accessed 5 September 2024).

[19] B. Alicona, "InfiniteFocus G6. Fast measurements for smooth surfaces & offline CAD planning.," Bruker Alicona. Accessed: June. 9, 2022. [Online]. Available: https://www.alicona.com/en/products/infinitefocus/.

[20] S.D. Mohanty, S.S. Mahapatra, R.C. Mohanty, J. Mohapatra, S.K. Khuntia, S. Nayak, Innovative methods of EDM electrode manufacturing: a review, Curr. Advan. Mech. Eng. (2021) 939–948, https://doi.org/10.1007/978-981-33-4795-3_87.

[21] N.H. Trieu, Electroplating of stereolithography printed part for sinker electrical discharge machining electrode fabricating. BachelorThesis, Vietnamese-German University, Germany, 2023 [Online]. Available: https://epub.vgu.edu.vn/handle/dlibvgu/1816. (Accessed 1 October 2024).

[22] X. Chen, Q. Cao, T. Chen, D. Wang, Y. Fan, W. Xing, 3D printing for precision construction of ceramic membranes: current status, challenges, and prospects, Advan. Membran. 3 (Jan. 2023) 100068, https://doi.org/10.1016/j.advmem.2023.100068.